Preparation and evaluation of micro and meso porous silica monoliths with embedded carbon nanoparticles for the extraction of non-polar compounds from waters

*Beatriz Fresco-Cala, Soledad Cárdenas, Miguel Valcárcel**

Department of Analytical Chemistry, Institute of Fine Chemistry and Nanotechnology, Marie Curie Building, Campus of Rabanales, University of Córdoba, 14071, Córdoba, Spain.

Abstract

A novel hybrid micro and meso porous silica monolith with embedded carbon nanoparticles (Si-CNPs monolith) was prepared inside a fused silica capillary (3 cm in length) and used as a sorbent for solid-phase microextraction. The hybrid monolithic capillary was synthetized by hydrolysis and polycondensation of a mixture of tetraethoxysilane (TEOS), ethanol, and three different carbon nanoparticles such as carboxylated single-walled carbon nanotubes (c-SWCNTs), carboxylated multi-walled carbon nanotubes (c-MWCNTs), and oxidized single-walled carbon nanohorns (o-SWNHs) via a two-step catalytic sol-gel process. Compared with silica monolith without carbon nanoparticles, the developed monolithic capillary column exhibited a higher extraction efficiency towards the analytes which can be ascribed to the presence of the carbon nanoparticles. In this regard, the best performance was achieved for silica monolith with embedded c-MWCNTs. The resulted monolithic capillaries were also characterized by scanning electron microscopy (SEM), elemental analysis and nitrogen intrusion porosimetry. Variables affecting to the preparation of the sorbent phase including three different carbon nanoparticles and extraction parameters were studied in depth using polycyclic aromatic hydrocarbons

(PAHs) as target analytes. Gas chromatography-mass spectrometry was selected as instrumental technique. Detection limits range from 0.1 to 0.3 $\mu g \cdot L^{-1}$, and the inter-extraction units precision (expressed as relative standard deviation) is between 5.9 and 14.4 %.

Keywords

Silica monolith, solid-phase microextraction, polycyclic aromatic hydrocarbons, carbon nanoparticles, monolithic hybrid solid.

*Corresponding author. Phone and fax: +34 957218616 email: qa1vacam@uco.es

1. Introduction

Polycyclic aromatic hydrocarbons (PAHs) are a group of non-polar organic compounds consisting of two or more benzene rings which are byproducts of petroleum processing or combustion of hydrocarbons. PAHs are of environmental concern due to their significant toxicity and potential carcinogenic properties at relatively low levels [1].In this regard, the concentration of benzo[a]pyrene has been used as indicator of total contamination by PAHs being 0.2 $\mu g \cdot L^{-1}$ the maximum level established by Agency for toxic substances & Disease Registry (ATSDR) in waters [2].

Analytical methods including gas chromatography (GC) [3], gas chromatography coupled with mass spectrometry (GC-MS) [4], high-performance liquid chromatography with fluorescence detection (HPLC-FLD) [5], thin-layer chromatography (TLC) [6], and spectrofluorimetry [7] have traditionally been used to determine PAHs. However, preconcentration and clean-up steps are needed to achieve the required sensitivity and selectivity. In this context, new microextraction techniques have been recently developed based on the simplification and the miniaturization of classical separation techniques in both solid and liquid phase formats. The incorporation of nanostructured materials as well as hybrid sorbents is behind the consolidation of these new approaches particularly due to their high superficial area and variety of interactions [8].

Monolithic solids have gained prominence as new separation material because of their unique properties including fast dynamic transport, simplicity of their preparation, frit-free construction, good loading capacity and low backpressure. To date, both organic polymer and silica-based monoliths have been used in several formats in the extraction context such

as micropipette-tips, spin columns, microfluidics chips, and capillary columns [9, 10]. Carbon nanoparticles, especially carbon nanotubes, have received special research attention since their discovery thanks to their unique and outstanding properties. Their excellent properties in terms of extraction efficiency have resulted in their use in different microextraction formats [11]. Hybrid monoliths prepared via sol-gel from silica precursors and organic frameworks including carbon nanoparticles combine the advantages of both [12-14]. The main challenge is to achieve a good and stable dispersion of the carbon nanoparticles in the polymerization mixture in order to obtain a homogeneous solid.

In this article, micro and meso porous silica monoliths with embedded carbon nanoparticles have been successfully synthesized inside a fused silica capillary and evaluated for the determination of non-polar compounds such as PAHs in tap and river water samples. Gas chromatography-mass spectrometry was selected as instrumental technique. All the variables related to the preparation of the monolith as well as those affecting to the microextraction process were evaluated in depth. In addition, the monolithic solid with and without carbon nanoparticles was characterized by elemental analysis to confirm their presence into the silica network and a porosimetry study was also carried out in order to know the size distribution of the pores.

2. Experimental section

2.1 Reagents, materials and samples

The reagents used were of analytical grade or better. Polycyclic aromatic hydrocarbons (naphthalene, phenanthrene, fluoranthene, pyrene, benz[a]anthracene and benzo[a]pyrene) were purchased from Sigma–Aldrich (Madrid, Spain. http://www.sigmaaldrich.com). Stock standard solutions of each analyte were prepared in methanol (Sigma-Aldrich) at a

concentration of 1 $g \cdot L^{-1}$ and stored at 4 ºC. Working solutions were prepared by dilution of the stocks in ultrapure Milli-Q water (Millipore Corp.; Madrid, Spain). In the extraction procedure, methanol from Sigma-Aldrich was employed as eluent.

Uncoated fused-silica capillaries (320 µm i.d., Sigma Aldrich) were used for the preparation of the monolithic extraction unit. Ferrules 1/16" ID, PEEK tubing 1/16" and internal union zero volume 1/16" to 1/16" (Sigma-Aldrich) were also employed.

The reagents needed for the synthesis of the monolithic phase, tetraethyl orthosilicate (TEOS), ethanol, Milli-Q water, 3-(trimethoxysilyl)propyl methacrylate, methanol, sodium hydroxide (NaOH), hydrochloric acid (HCl), acetone and acetic acid were purchased from Sigma-Aldrich.

Carboxylated multi-walled carbon nanotubes (c-MWCNTs, < 8 nm o.d., 10-30 µm length, > 95 wt% purity, 3.86 wt% functional content) and carboxylated single-walled carbon nanotubes (c-SWCNTs, 1-2 nm o.d., 5-30 µm length, >90 wt% purity, 2.73 wt% functional content) were obtained from Sigma-Aldrich. Single-walled nanohorns were purchased from Carbonium S.r.l (Padua, Italy. http://www.carbonium.it/public/site/index.php). SWNHs form stable dahlia-shaped aggregates with an average diameter of 60-80 nm. Individually, the lengths of these SWNHs are in the range of 40 to 50 nm, and the diameter in the cylindrical structure varies between 4-5 nm.

The dispersions of the carboxylated carbon nanotubes (c-SWCNTs and c-MWCNTs) were made in ethanol. In brief, 5 mg of c-MWCNTs were weighed, added to a glass vial and ultrasonic-assisted dispersed in 50 mL of ethanol for 30 min. On the other hand, carbon nanohorns (SWNHs) were weighed (5 mg) and added to a glass vial, which was further introduced into a microwave oven, being the solid irradiated at 800 W for 10 min. After

cooling at room temperature, the oxidized carbon nanohorns (o-SWNHs) were dispersed in 50 mL of ethanol and sonicated for 30 min.

Tap and river water samples were selected for the determination of the target compounds using the monolithic microextraction unit. Water samples from the Guadalquivir river were collected in amber glass bottles without headspace. The spiked samples were prepared by adding the analytes at a concentration of 20 $\mu g \cdot L^{-1}$, and then they were left to stand for 24 h until the analysis.

2.2 Chromatographic analysis

Gas chromatographic/mass spectrometric analyses were carried out on a gas chromatograph (Varian CP-3800)-mass spectrometer (Varian 1200 MS/MS) working under single quadrupole mode and with an electron multiplier detector. The gas chromatograph was equipped with a fused silica capillary column VF-5 ms (30 m x 0.25 mm i.d.) coated with 5 % phenyl-95 % dimethylpolysiloxane (film thickness 0.25 μm) (Sigma-Aldrich) to separate the six analytes. System control and data acquisition was achieved with an HP1701CA MS ChemStation software.

The column temperature program was as follows: the initial temperature, 80 ºC, was kept for 2.5 min, raised up to 200 ºC at 25 $°C \cdot min^{-1}$ (maintained for 1 min) and further to 250 ºC at 10 $ºC \cdot min^{-1}$. Then it was immediately ramped up to 285 ºC at 5 $ºC \cdot min^{-1}$. The final temperature, 300 ºC, was reached with a ramp of 30 $ºC \cdot min^{-1}$ and maintained for 1 min. The quadrupole mass spectrometer detector was operated in selected ion monitoring mode, recording the following fragment-ions characteristic of each analyte: 128 (from 3.0 to 6.4 min) for naphthalene, 178 (from 6.4 to 10.58 min) for phenanthrene, 202 (from 10.58 to

14.0 min) for fluoranthene and pyrene, 228(from 14.0 to 17.0 min) for benz[a]anthracene, 252 (from 17.0 to 21.0 min) for benzo[a]pyrene, all of them at 1 scan/s. Electron impact ionization (70 eV) was used for analytes fragmentation. The injector temperature was 270 ºC and the splitless mode was selected. The injection volume, 2 μL of methanol, was measured with a 5 μL microsyringe (Hamilton Co., Nevada, USA). The carrier gas used was helium (6.0 grade, Air Liquide, Seville, Spain) at a flow rate of 1.0 $mL \cdot min^{-1}$, and it was regulated by digital pressure controller. The transfer line and ionization source were maintained at 280 ºC and 250 ºC, respectively.

2.3 Preparation of Si-CNPs monolithic solid

It is well known that silica monoliths tend to shrink during the post-heat treatment, even in small devices such as capillaries. However, this shrinkage can be minimized or prevented by a covalent attachment of the monolith to the capillary inner walls. Therefore, the hybrid monolith was synthetized inside a fused silica capillary (3 cm in length) which was previously modified with 7% solution of 3-(trimethoxysilyl)propyl methacrylate in ethanol [15].

A schematic representation of the synthesis procedure is shown in the Fig. 1. The hybrid monolith was prepared by hydrolysis and polycondensation of precursors via a two-step catalytic sol-gel process according to a previously described procedure with some modifications [16]. It should be noticed that the rate of hydrolysis and condensation of the precursors is the most important factor to control the final monolithic structure. The kinetics of each step of the sol-gel process is pH-dependent. Low pH values produce a fast hydrolysis of alkoxysilanes generating hydroxyl groups, while high pH values accelerate the condensation reactions [16]. This pH variation was regulated by adding hydrochloric

156 acid (0.5 M) or ammonium hydroxide (0.5 M) as required In the acid-catalyzed hydrolysis
157 step, 160 μL of the TEOS was mixed with a solution of 200 μL of ethanol containing one
158 of the three carbon nanoparticles studied (0.1 $g \cdot L^{-1}$), 20 μL of Milli-Q water, and 10 μL of
159 HCl (0.5 M) in a 1.5 mL eppendorf vial. The pre-polymerization mixture solution was
160 sonicated at 20 ºC for 4 h, and then 25 μL of ammonium (0.5 M) were added into the
161 solution. After shaking the mixture, the modified capillaries were filled with the
162 homogenous polymerization mixture up to a length of 3 cm, and sealed at both ends with
163 two pieces of rubbers. Next, the capillaries were introduced into an oven at 40 °C for 12 h.
164 After polymerization and using a micro-HPLC pump, the resulting columns were rinsed
165 with ethanol to remove any possible unreacted monomer and the soluble hydrolysis
166 products. Then, the monolithic capillary was flushed with a 5 % (v/v) solution of acetic
167 acid in methanol for 10 min (0.1 $mL \cdot min^{-1}$), followed by Milli-Q water (0.1 $mL \cdot min^{-1}$, 10
168 min) in order to conditioning the surface monolith prior to use.
169
170 *2.4 Characterization*
171 A JEOL JSM 6300 scanning electron microscopy (Isaza, Alcobendas, Spain) was also used
172 to obtain the micrographs of the monolithic solid with and without carbon nanoparticles to
173 evaluate the morphological and structural characteristics of the monolithic sorbent. The
174 monolith was fixed on the stub by a double-sided sticky tape and then coated with gold.
175 Transmission electron microscopy (TEM) images were recorded by use of a JEOL JEM
176 1400 microscope (Isaza, Alcobendas, Spain) operating at an accelerating voltage of 120
177 kV. The TEM micrographs were used to characterize the nanoparticles size and
178 morphology.

Elemental analysis was carried out on an elemental analyzer CHNS Eurovector EA 3000. Nitrogen adsorption/desorption experiments were carried out at -196 ºC using a Quantachrome® ASiQwin™-Automated Gas Sorption Data. The specific surface area values were calculated according to the BET (Brunauer–Emmett–Teller) equation. T-plot method was used to determine the micropore surface areas, and the average pore volumes were evaluated from the desorption branches of isotherms based on the BJH (Barrett–Joyner–Halenda) model.

2.5 Analytical procedure

The microextraction procedure followed for the isolation and preconcentration of PAHs from waters comprised the following steps. First, aliquots of 2 mL of aqueous standards or water samples, containing the target analytes, were passed through the polymer monolithic capillary at a flow rate of 0.1 $mL \cdot min^{-1}$ by means of the micro-HPLC pump. The monolith was washed with 500 µL of Milli-Q water (0.1 $mL \cdot min^{-1}$), and then the aqueous phase remaining in the capillary was eliminated by means of a nitrogen stream (10 min). After this step, the analytes were eluted pumping methanol (500 µL, 0.1 $mL \cdot min^{-1}$), and the eluent was collected into a vial, evaporated and the residue was redisolved in 10 µL of methanol. Finally, 2 µL of the organic phase with the extracted analytes were analyzed by GC/MS. The chromatographic peak areas were used as analytical signals. Between extractions, the monolith was sequentially conditioned with a 5 % (v/v) solution of acetic acid in methanol and Milli–Q water (10 min in each case) at a flow rate of 0.1 $mL \cdot min^{-1}$. No degradation effects or deformation of the monolithic structure was observed in terms of extraction efficiency with repetitive microextraction cycles. The extraction unit can be used repeatedly owing to its compatibility with organic solvents as well as water [17].

3. Results and discussion

3.1 Variables affecting to the preparation of the monolith

The preparation of the bare monolith was carried out as described in section 2.3. The incorporation of carbon nanoparticles (c-SWCNTs, c-MWCNTs and o-SWNHs) in the monolith was deeply studied. As it was previously mentioned, the homogenous and stable dispersion of the nanoparticles is crucial for this aim. Therefore, dispersions of each carbon nanoparticle were prepared at a concentration of 0.1 $g \cdot L^{-1}$ and several organic solvents (methanol, ethanol and 2-propanol) were studied to efficiently disperse the carbon nanoparticles. Fig. 2 shows the behavior for each carbon nanoparticle in the different organic media. As it can be seen, ethanol resulted to be the best choice to disperse the carboxylated carbon nanotubes (Fig. 2A and 2B), while good dispersion of o-SWNHs was obtained in the three solvents (Fig. 2C). Therefore, ethanol was selected as optimum solvent for the efficient dispersion of the carbon nanoparticles used in this article. Fig. 2D also presents the TEM micrographs obtained for the dispersions of c-SWCNTs, c-MWCNTs, and o-SWNHs.

Next, the influence of these carbon nanoparticles incorporated to the monolith was evaluated in terms of extraction efficiency using aqueous standards containing benzo[a]pyrene as model compound at a concentration of 1 $\mu g \cdot mL^{-1}$. As it can be seen in Fig. 3, the introduction of the c-MWCNTs, c-SWCNTs, and o-SWNHs into the network of silica monoliths improved the extraction of benzo[a]pyrene in comparison with the bare monolith. In fact, the best performance was achieved using c-MWCNTs due to their large specific surface area and number of sheets. On the other hand, o-SWNHs present an extensive surface area and horn interstices which provide them with an exceptional adsorption capacity. Besides, the oxidation conditions can produce nanowindows,

generating additional interaction sites on the conical and curved ends. All this, combined with the formation of stable aggregates improve their extraction capacity explaining the better performance in comparison with c-SWCNTs. Based on the results obtained, this, c-MWNTs were selected for further experiments. Next, the amount of c-MWCNTs was evaluated at concentrations of 0.01, 0.05 and 0.1 $g \cdot L^{-1}$. Monolithic solid formed at concentrations of nanoparticles higher than 0.1 $g \cdot L^{-1}$ showed non homogenous distribution of the c-MWCNTs due to the aggregation of the carbon nanoparticles decreasing the extraction efficiency. As it is shown in Fig. 4, the signals increased with the concentration, and therefore a concentration of 0.1 $g \cdot L^{-1}$ of the c-MWCNTs in ethanol was selected.

3.2 Characterization

Once optimized, the synthetized monoliths were characterized by SEM, elemental analysis, and nitrogen adsorption/desorption measurements.

Micrographs of the monolithic sorbents were obtained for the bare silica, Si-SWNHs, Si-SWCNTs, and Si-MWCNTs monolith. As it can be seen in the Fig. 5, the silica monolithic solids exhibit homogeneous and porous networks that consisted of interconnected microglobules. It is worth to mention that the graph of the Si-SWNHs monolith (Fig. 5B) shows that SWNHs form spherical aggregates with dahlia-like structures, while the monolithic solids modified with carbon nanotubes (Fig. 5C and 5D) maintain practically the same microscopic morphology as it showed for the bare silica monolith (Fig. 5A).

The C% of the bare silica, Si-SWNHs, Si-SWNCTs, and Si-MWCNTs monolith was determined by elemental analysis and resulted to be 0.72%, 4.24%, 1.94%, and 2.48%, respectively. The increase in the proportion of the carbon in the synthetized material demonstrated the successful incorporation of the carbon nanoparticles into the silica

250 network. As expected, the highest percentage was found for the single walled carbon
251 nanohorns due to its size and weight.
252 Isotherms of nitrogen adsorption/desorption for each type of synthetized monolithic solid
253 are described in Fig 6. As it can be seen, the isotherms for silica, Si-SWNHs, and Si-
254 SWCNTs monoliths were type I in the BDDT classification [18], while the nitrogen
255 isotherms obtained for the Si-MWCNTs monolith was the type IV, exhibiting H1 hysteresis
256 loops which indicates a mesoporous solid. The BET surface and pore volume values are
257 compiled in the Table 1 together with the micropore surface areas.
258
259 *3.3 Evaluation of the variables affecting to the microextraction process*
260 As it is a novel extraction procedure, an univariate approach was selected to study the effect
261 of each single variable in the extraction process, using aqueous standards containing
262 benzo[a]pyrene as model compound at a concentration of 1 $\mu g \cdot mL^{-1}$. The initial
263 experimental conditions for the microextraction process were: 3 mL of aqueous standard
264 and an elution volume of 200 µL of methanol. Flow rates used for preconcentration and
265 elution step were fixed at 0.1 $mL \cdot min^{-1}$.
266 The sample and eluent volumes are critical parameters for the method sensitivity, since they
267 will determine the preconcentration factor. The sample volume was studied within the
268 interval 1-4 mL. The maximum extraction efficiency for the target triazines was achieved
269 for a volume of 2 mL, decreasing over this value due to a breakthrough effect. The volume
270 of methanol required for analytes elution was studied between 100 and 500 µL. The
271 methanolic extract was collected in a 1.5 mL glass vial, and a volume of 500 µL was
272 necessary to quantitatively elute the target analytes which was fixed as optimum. An
273 evaporation–redissolution step was included in order to reduce the final volume to 10 µL,

thus increasing the method sensitivity. Finally, 2 μL of the organic phase with the extracted analytes were injected into the gas chromatograph/mass spectrometer for their separation and detection. The chromatographic peak areas were used as analytical signals.

Between samples, the monolithic capillary was conditioned with a 5 % (v/v) solution of acetic acid in methanol for 10 min. The pH of the solvent is a critical parameter in the conditioning in order to achieve a reproducible elution as underivatized silica exhibit secondary interactions between analytes and negative charged silanol groups at pH >4 [19]. Milli–Q water was sequentially passed through the hybrid monolithic capillary at a flow rate of 0.1 $mL \cdot min^{-1}$ for 10 min.

*3.4 Analytical figures of merit and analysis of water samples*The analytical figures of merit of the proposed method are summarized in Table 2. The calibration curves for PAHs was constructed by using working aqueous standards prepared in duplicate at controlled concentrations which were subjected to the optimized extraction procedure, and 2 μL of the organic extract was injected into the GC/MS for analysis. The corresponding equations were obtained by plotting the peak areas of the characteristic m/z fragment ions against the concentration for each target analyte. The method was characterized on the basis of its linearity, sensitivity, and precision.

The corresponding calibration graphs were constructed by extracting in duplicate nine working aqueous standards containing the analytes at concentrations in the range from 0.3 to 1000 $\mu g \cdot L^{-1}$. The sensitivity of the method was evaluated according to the limit of detection (LOD) and quantification (LOQ). LODs, calculated by using a signal-to-noise ratio (S/N) of 3, were 0.1 $\mu g \cdot L^{-1}$ and the LOQs, calculated by using a S/N of 10, were 0.3 $\mu g \cdot L^{-1}$ for all analytes. The linearity was maintained at least in the interval 0.3-1000 $\mu g \cdot L^{-1}$

298 for all analytes. Figure 7 shows a SIM chromatograph with the different m/z fragments ions
299 obtained after monolithic microextraction procedure of a blank water and a standard sample
300 with the target analytes at 0.1 $\mu g \cdot L^{-1}$.The precision of the method was studied under
301 repeatability and reproducibility experimental conditions. Repeatability (intra-extraction
302 units conditions), expressed as relative standard deviation (RSD) was calculated from five
303 individual standards prepared at a concentration of 1 $\mu g \cdot mL^{-1}$ and it was lower than 14.1 %
304 for all the analytes. The reproducibility between extraction units (inter-extraction units) was
305 also evaluated and the results, expressed as RSD (n=5) ranged from 5.9 to 14.4 %.
306 Once optimized and analytically characterized, the proposed method was applied to the
307 determination of the target PAHs in environmental water samples (tap and river). The
308 samples were analyzed in order to find any potential presence of the analytes. Since the
309 analytes were not detected, validation samples were prepared using blank waters samples
310 (tap and river waters) fortified with the six target analytes (naphthalene, phenanthrene,
311 fluoranthene, pyrene, benz[a]anthracene and benzo[a]pyrene) at a concentration of 20 $\mu g \cdot L^{-1}$
312 . Samples were maintained in amber glass bottles without headspace and in the dark for 24
313 h until analysis. Then, the fortified samples were analyzed using the extraction method, and
314 the concentration for each PAH was calculated by interpolating the peak area obtained in
315 the corresponding calibration graph. The recovery values were calculated dividing the
316 concentration found by the concentration added, and expressed in percentage. The recovery
317 values (average of three replicates) obtained for each of the fortified samples analyzed are
318 shown in Table 3, and they ranged from 72 to 124 %.
319

320 **4. Conclusions**

In this study, a novel silica monolith with embedded carbon nanoparticles was synthetized inside a fused silica capillary for the extraction of non-polar compounds from water samples. The hybrid monolithic solid sorbent was prepared by two-step catalytic sol-gel process and the NPs were directly added into the polymerization mixture. The most critical point of the synthesis was to achieve stable dispersions of the NPs due to their tendency to form aggregates over time. A comparison between the silica monolith without and with carbon nanoparticles was carried out. Hence, the three selected NPs were evaluated as sorbents improving the extraction capacity in any case. Among them, the best results were obtained for the c-MWCNTs being selected as optimum. Variables affecting to the preparation of the monolithic solid as well as the extraction conditions were evaluated by optimizing experimental parameters.

This work, demonstrates that the addition of the carbon NPs into silica solid monolithic significantly increases the extraction efficiency for the target analytes due to π-π stacking interaction and hydrophobic effect. In addition, the proposed microextraction method shows favorable analytical features in comparison to the previously reported analytical methods for the determination of PAHs in water samples. By way of example, Table 4 summarizes the main analytical information of the selected references related to the proposed microextraction method, including LODs and LOQs as well as extraction format used. As it can be derived from the data shown in the table, the proposed method presents similar limits of quantification compared with the majority of the other approaches. The lowest LOQs were obtained for [21], were an on-line thermal desorption step of the retained analytes was implemented. This fact dramatically improves the method sensitivity as it avoids the dilution inherent to the chemical elution. Also, the inclusion of the fluorimetic detection resulted in a better sensitivity thanks to the native fluorescence of

PAHs. Nevertheless, it should be highlighted that present hybrid sorbent has been optimized for achieve the concentration level established by ATSDR, and therefore, a better sensitivity is not required in water samples.

Acknowledgments

Financial support from the Spanish Ministry of Science and Innovation (CTQ2014-52939-R) is gratefully acknowledged. B. Fresco-Cala expresses her gratitude for the predoctoral grant (ref FPU13/03896) from the Spanish Ministry of Education. The authors would like to thank the Central Service for Research Support (SCAI) of the University of Córdoba for the service provided to obtain the micrographs and elemental analysis measurements.

Figures

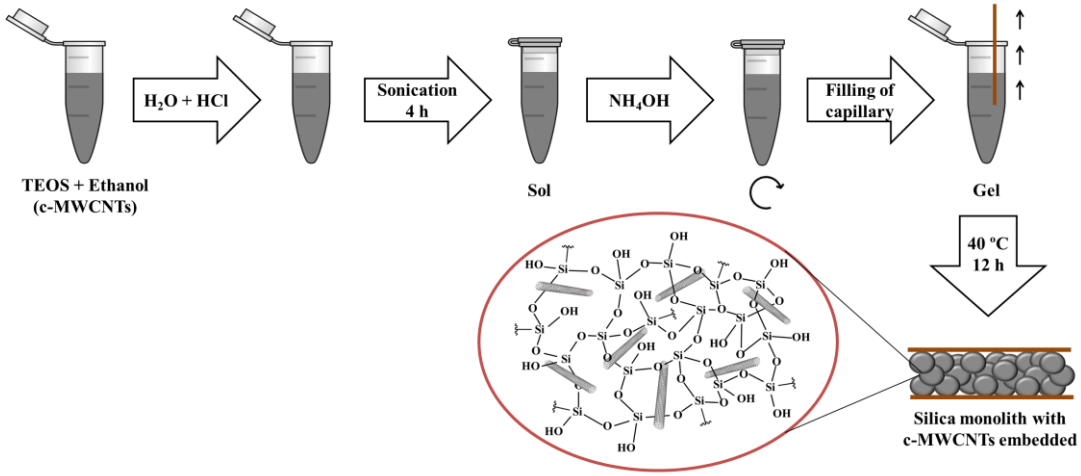

Fig. 1 Scheme of the sol-gel process and the filling of the fused silica capillary.

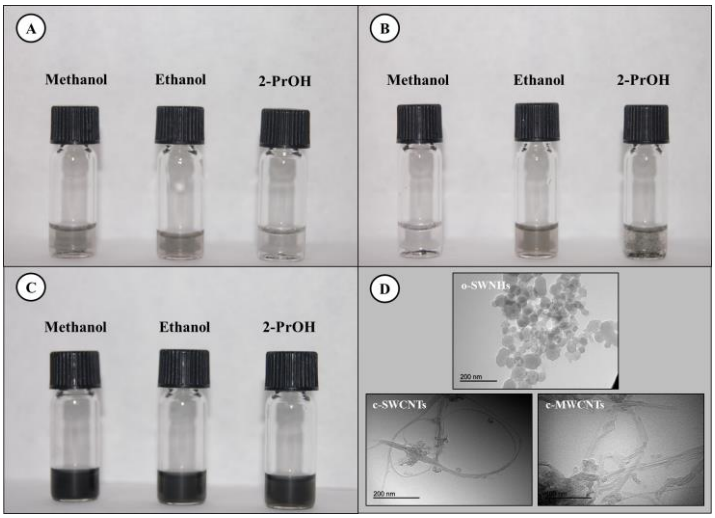

Fig. 2 Photographs of the dispersions of c-SWCNTs (A), c-MWCNTs (B), and o-SWNHs (C) in methanol, ethanol, and 2-PrOH; and TEM images (D) of the three carbon nanostructures.

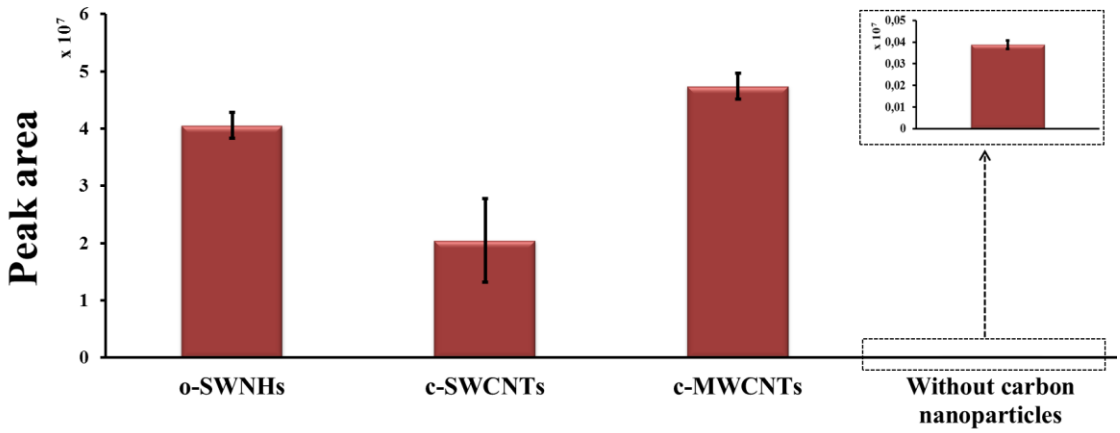

375

376 Fig. 3 Comparison of the analytical performance of silica monolith without nanoparticles

377 and the monolith containing embedded o-SWNHs, c-SWCNTs and c-MWCNTs.

378

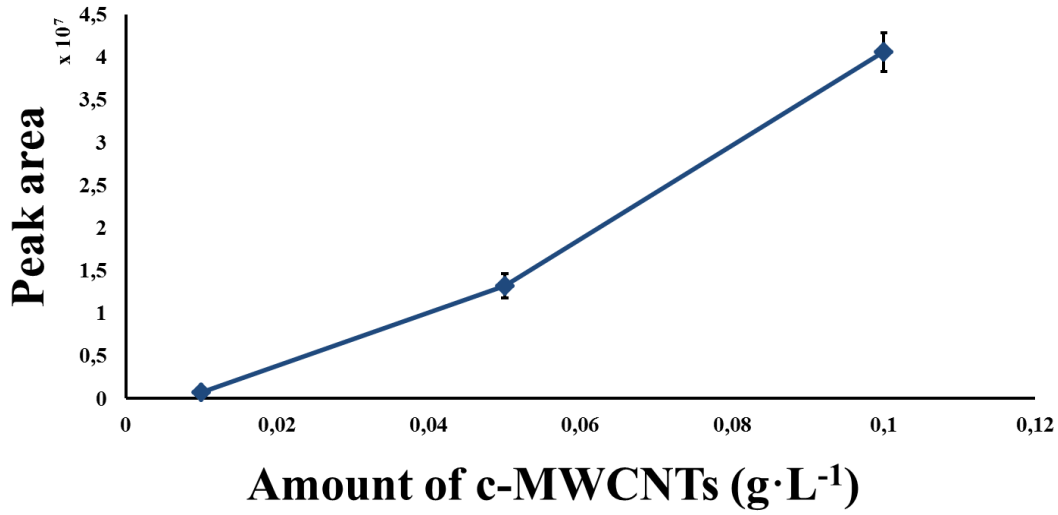

379

380 Fig. 4 Influence of the concentration of the c-MWCNTs dispersion on the PAHs retention.

381

382

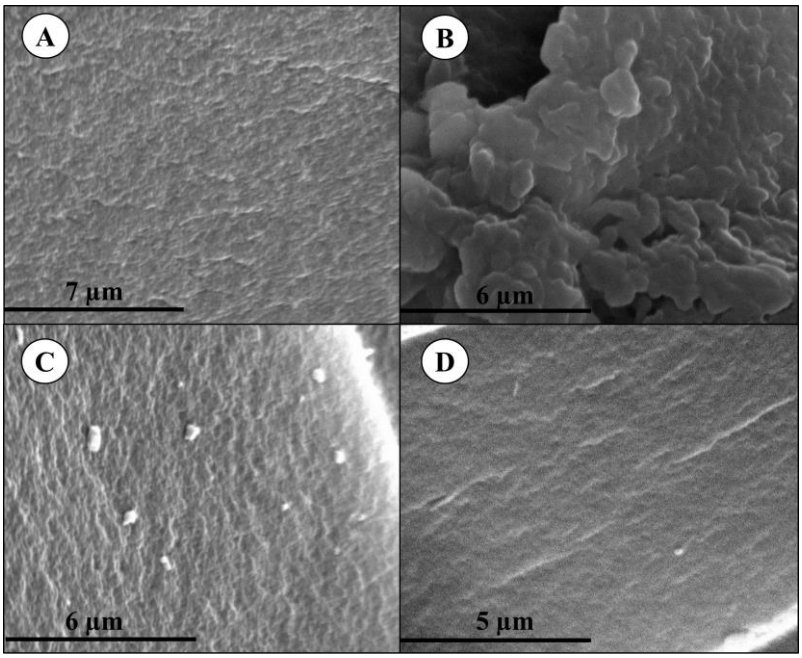

Fig. 5 Scanning electron microscopy of silica monolith (A), Si-SWNHs (B), Si-SWCNTs (C), and Si-MWCNTs (D).

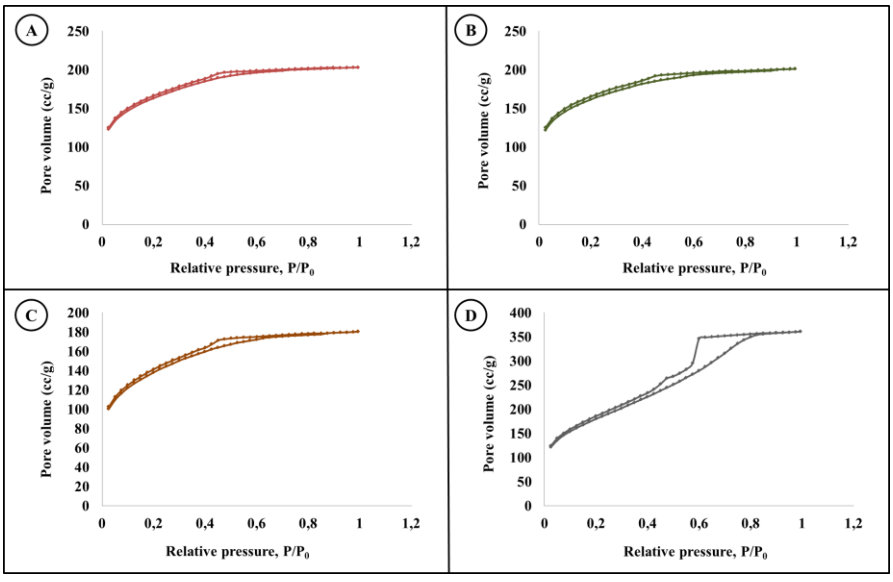

Fig. 6 N_2 adsorption and desorption isotherms of silica monolith (A), Si-SWNHs (B), Si-SWCNTs (C), and Si-MWCNTs (D). P: sample pressure; Po: saturation pressure.

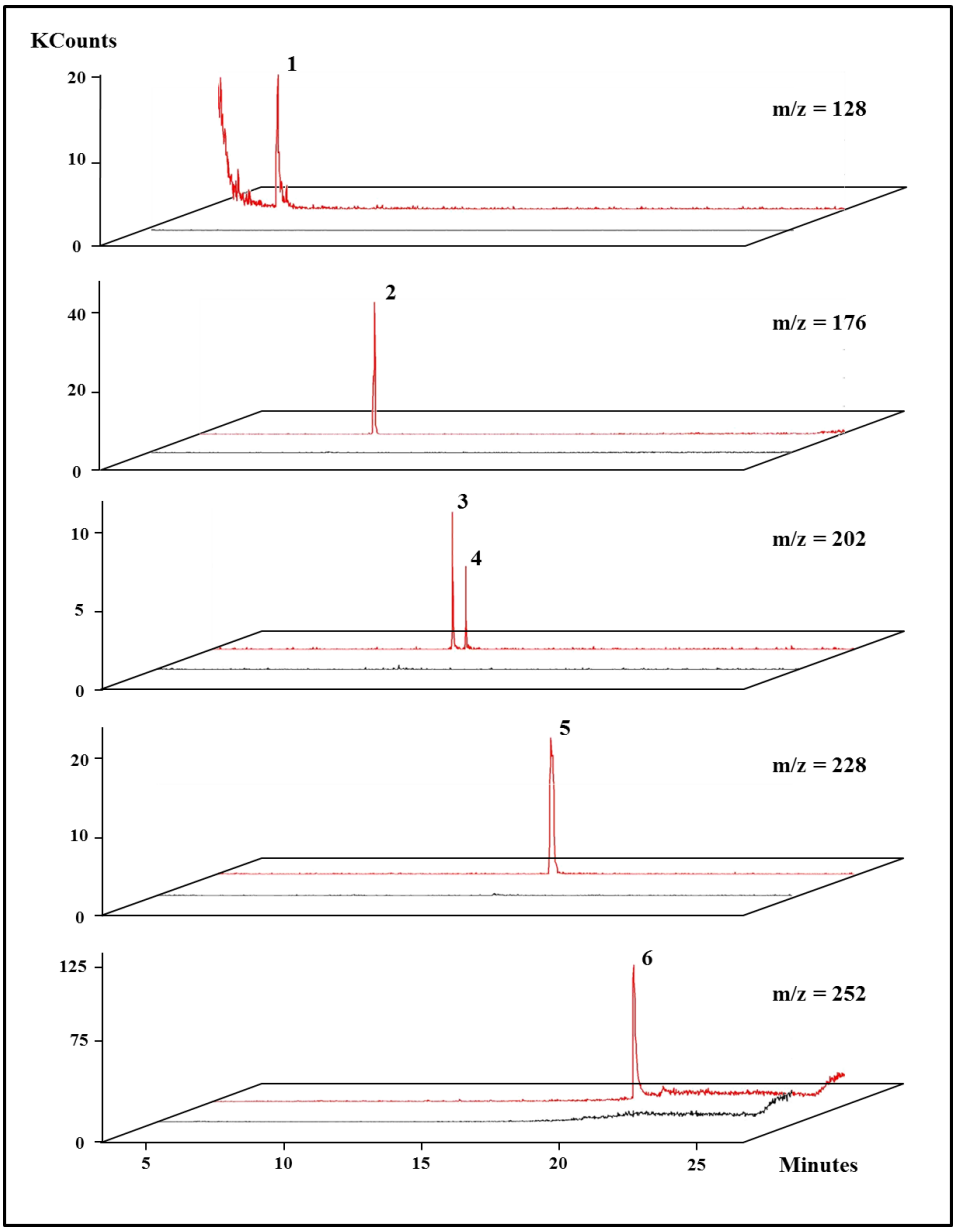

391

392 Fig. 7 SIM chromatogram obtained after monolithic microextraction procedure of a blank

393 water (green) and a standard sample with the target analytes at 0.1 $\mu g \cdot L^{-1}$ (red). Peaks: (1)

394 Naphthalene, (2) Phenantrene, (3) Fluoranthene, (4) Pyrene, (5) Benz[a]anthracene, (6)

395 Benzo[a]pyrene.

396

397

Table 1. Textural properties of the synthetized monolithic solids.

	Silica monolith	**Si-SWNHs monolith**	**Si-SWCNTs monolith**	**Si-MWCNTs monolith**
Specific surface area, BET (m^2/g)	594.07	588.25	497.37	646.82
Micropore surface area (m^2/g)	345.41	352.80	255.52	108.89
Average pore volume (cc/g)	0.314	0.311	0.279	0.557

Table 2. Analytical figures of merit of Si-MWCNTs monolithic microextraction unit to the determination of the target polycyclic aromatic hydrocarbons.

Analyte	m/z	LOD ($\mu g \cdot L^{-1}$)	LOQ ($\mu g \cdot L^{-1}$)	Precision	
				Intra-extraction units RSD (%, n=5)	Inter-extraction units RSD (%, n=5)
Naphthalene	128	0.1	0.3	14.1	12.9
Phenanthrene	178	0.1	0.3	10.2	14.4
Fluoranthene	202	0.1	0.3	8.8	10.9
Pyrene	202	0.1	0.3	8.4	7.9
Benz[a]anthracene	228	0.1	0.3	10.8	10.7
Benzo[a]pyrene	252	0.1	0.3	13.3	13.9

412 *Table 3. Recovery study for naphthalene, phenanthrene, fluoranthene, pyrene,*
413 *benz[a]anthracene, and benzo[a]pyrene spiked to water samples analyzed following Si-*
414 *MWCNTs monolithic extraction unit.*

Analyte	Tap water (%, n=3)	River water (%, n=3)
Naphthalene	113 ± 7	105 ± 5
Phenanthrene	85 ± 11	82 ± 14
Fluoranthene	99 ± 9	76 ± 9
Pyrene	101 ± 8	72 ± 8
Benz[a]anthracene	124 ± 5	121 ± 10
Benzo[a]pyrene	114 ± 14	109 ± 14

415
416
417
418
419
420
421
422
423
424

Table 4. Comparison of the developed Si-CNPs monolith with other monolithic solids reported for the determination of PAHs.

Monolithic sorbent	Selected PAHs	Packing	Sample	LODs	LOQs	Detection	Reference
Si-CNPs monolith	Naphthalene, phenanthrene, fluoranthene, pyrene, benz[a]anthracene, and benzo[a]pyrene	Monolithic capillary column	Water samples	0.1 μg·L^{-1}	0.3 μg·L^{-1}	GC-MS	This work
Molecularly imprinted sol-gel polymer	Naphthalene, acenaphthylene, acenaphthene, fluorene, phenanthrene, anthracene, fluoranthene, pyrene, benz[a]anthracene, chrysene, benzo[b]fluoranthene, benzo[k] fluoranthene, benzo[a]pyrene, indeno[1,2,3-cd]pyrene, dibenz[a,h]anthracene, and benzo[ghi]perylene	Packed SPE	Water samples	5.2-12.6 ng·L^{-1}	0.10-1.0 μg·L^{-1}	GC-MS	[20]
Poly(butyl methacrylate-*co*-ethylene dimethacrylate) monolith	Naphthalene, acenaphthene, fluorene, anthracene, fluoranthene, pyrene, benz[a]anthracene, benzo[k], fluoranthene, benzo[a]pyrene, and indeno[1,2,3-cd]pyrene	Monolithic capillary column	Water samples	2.8-11.5 ng·L^{-1}	0.012-0.05 μg·L^{-1}	GC-MS	[21]
Graphene monolith	Naphthalene, acenaphthene, fluorene, phenanthrene, fluoranthene, pyrene, and benz[a]anthracene	Monolithic fiber	Water samples	4.0-50.0 ng·L^{-1}	0.05-0.5 μg·L^{-1}	GC	[22]
Hybrid organic-inorganic	Biphenyl, fluorene, phenanthrene, and fluoranthene	Monolithic capillary column	Water samples	2.4-8.1 μg·L^{-1}	8.0-27.8 μg·L^{-1}	μ-HPLC-UV	[23]
Poly(vinylpyrrolidone-*co*-divinylbenzene)	Naphthalene, fluorene, and fluoranthene	Stir bar	Water samples	0.045-0.093 μg·L^{-1}	-	GC-MS	[24]
PolyHIPE monolith	Naphthalene, acenaphthylene, acenaphthene, fluorene, phenanthrene, anthracene, fluoranthene, pyrene, benz[a]anthracene, chrysene, benzo[b]fluoranthene, benzo[k]fluoranthene, benzo[a]pyrene, dibenz[a,h]anthracene, and benzo[ghi]perylene	Pipette tips	Water samples	0.004-0.228 ng·L^{-1}	0.1-1.0 μg·L^{-1}	HPLC-FLD	[25]

References

[1] N. Aguinaga, N. Campillo, P. Vinas, M. Hernández-Córdoba, Determination of 16 polycyclic aromatic hydrocarbons in milk and related products using solid-phase microextraction coupled to gas chromatography–mass spectrometry, Anal. Chim. Acta, 596 (2007) 285-290.

[2] [ATSDR] Agency for Toxic Substances and Disease Registry. Toxicological profile for polycyclic aromatic hydrocarbons (PAHs). http://www.atsdr.cdc.gov/csem/pah (accessed 01.04.16)

[3] A. Amiri, M. Baghayeri, M. Kashmari, Magnetic nanoparticles modified with polyfuran for the extraction of polycyclic aromatic hydrocarbons prior to their determination by gas chromatography, Microchim. Acta, 183 (2016) 149-156.

[4] X. Ruan, Q. Lu, Z. Yang, Analytical method development for determining polycyclic aromatic hydrocarbons and organophosphate esters in indoor dust based on solid phase extraction and gas chromatography/mass spectrometry, Anal. Methods, 8 (2016) 1690-1698.

[5] Z. Taghvaee, Z. Piravivanak, K. Rezaei, M. Faraji, Determination of Polycyclic Aromatic Hydrocarbons (PAHs) in Olive and Refined Pomace Olive Oils with Modified Low Temperature and Ultrasound-Assisted Liquid–Liquid Extraction Method Followed by the HPLC/FLD, Food Anal. Methods, (2015) 1-8.

[6] K. Tyrpieñ, M. Szumska-Kostrzewska, C. Dobosz, Optimisation of densitometric fluorescence detection conditions of selected carcinogenic compounds in planar chromatography, Chemia analityczna, 52 (2007) 749-756.

[7] P. Rodríguez-Sanmartín, A. Moreda-Piñeiro, A. Bermejo-Barrera, P. Bermejo-Barrera, Ultrasound-assisted solvent extraction of total polycyclic aromatic hydrocarbons from mussels followed by spectrofluorimetric determination, Talanta, 66 (2005) 683-690.

[8] B. Fresco-Cala, J.M. Jimenez-Soto, S. Cardenas, M. Valcarcel, Single-walled carbon nanohorns immobilized on a microporous hollow polypropylene fiber as a sorbent for the extraction of volatile organic compounds from water samples, Microchim. Acta, 181 (2014) 1117-1124.

[9] X. Huang, D. Yuan, Recent developments of extraction and micro-extraction technologies with porous monoliths, Crit. Rev. Anal. Chem., 42 (2012) 38-49.

[10] L. Xu, Z.-G. Shi, Y.-Q. Feng, Porous monoliths: sorbents for miniaturized extraction in biological analysis, Anal. Bional. Chem., 399 (2011) 3345-3357.

[11] B. Socas-Rodríguez, A.V. Herrera-Herrera, M. Asensio-Ramos, J. Hernández-Borges, Recent applications of carbon nanotube sorbents in analytical chemistry, J. Chromatogr. A, 1357 (2014) 110-146.

[12] M.-M. Zheng, S.-T. Wang, W.-K. Hu, Y.-Q. Feng, In-tube solid-phase microextraction based on hybrid silica monolith coupled to liquid chromatography–mass spectrometry for automated analysis of ten antidepressants in human urine and plasma, J. Chromatogr. A, 1217 (2010) 7493-7501.

[13] J. Hu, X. Li, Y. Cai, H. Han, Hybrid silica polymeric monolith-based in-tube microextraction and CE for determination of bisphenol A in beverages, J. Sep. Sci., 32 (2009) 2759-2766.

[14] J. Ou, H. Lin, Z. Zhang, G. Huang, J. Dong, H. Zou, Recent advances in preparation and application of hybrid organic-silica monolithic capillary columns, Electrophoresis, 34 (2013) 126-140.

475 [15] B. Fresco-Cala, S. Cárdenas, M. Valcárcel, Improved microextraction of selected
476 triazines using polymer monoliths modified with carboxylated multi-walled carbon
477 nanotubes, Microchim. Acta, 183 (2016) 465-474.
478 [16] W. Zhang, Y. Feng, L. Zhang, T. Li, Y. Zhang, Hybrid organic–inorganic phenyl
479 monolithic column for capillary electrochromatography, Electrophoresis, 26 (2005) 2935-
480 2941.
481 [17] P.D. Fletcher, S.J. Haswell, P. He, S.M. Kelly, A. Mansfield, Permeability of silica
482 monoliths containing micro-and nano-pores, J. Porous Mater., 18 (2011) 501-508.
483 [18] S. Brunauer, L.S. Deming, W.E. Deming, E. Teller, On a theory of the van der Waals
484 adsorption of gases, J. Am. Chem. Soc., 62 (1940) 1723-1732.
485 [19] T. Nema, E. Chan, P. Ho, Application of silica-based monolith as solid phase
486 extraction cartridge for extracting polar compounds from urine, Talanta, 82 (2010) 488-
487 494.

488 [20] X. Song, J. Li, S. Xu, R. Ying, J. Ma, C. Liao, D. Liu, J. Yu, L. Chen, Determination
489 of 16 polycyclic aromatic hydrocarbons in seawater using molecularly imprinted solid-
490 phase extraction coupled with gas chromatography-mass spectrometry, Talanta, 99 (2012)
491 75-82.

492 [21] F. Galán-Cano, V. Bernabé-Zafón, R. Lucena, S. Cárdenas, J.M. Herrero-Martínez, G.
493 Ramis-Ramos, M. Válcarcel, Sensitive determination of polycyclic aromatic hydrocarbons
494 in water samples using monolithic capillary solid-phase extraction and on-line thermal
495 desorption prior to gas chromatography–mass spectrometry, J. Chromatogr. A, 1218 (2011)
496 1802-1807.

[22] J. Fan, Z. Dong, M. Qi, R. Fu, L.Qu, Monolithic graphene fibers for solid-phase microextraction, J. Chromatogr. A, 1320 (2013) 27-32.

[23] M.M. Zeng, B. Lin, Y.Q. Feng, Hybrid organic–inorganic octyl monolithic column for in-tube solid-phase microextraction coupled to capillary high-performance liquid chromatography, J. Chromatogr. A, 1164 (2007) 48-55.

[24] X. Huang, N. Qiu, D. Yuan, B. Huang, A novel stir bar sorptive extraction coating based on monolithic material for apolar, polar organic compounds and heavy metal ions, Talanta, 78 (2009) 101-106.

[25] R. Su, G. Ruan, H. Nie, T. Xie, Y. Zheng, F. Du, J. Li, Development of high internal phase emulsion polymeric monolithsfor highly efficient enrichment of trace polycyclic aromatichydrocarbons from large-volume water samples, J. Chromatogr. A, 1405 (2015) 23-31